An experimental approach for investigating scuffing initiation due to overload cycles with twin-disc test device

Published article can be found at: https://doi.org/10.1016/j.triboint.2017.01.005

An experimental approach for investigating scuffing initiation due to overload cycles with a twin-disc test device

Matti Savolainen, Arto Lehtovaara
Group of Tribology and Machine Elements
Department of Materials Science, Tampere University of Technology
PO BOX 589, 33101 Tampere, Finland

Abstract

This paper presents an investigation into the effect of unexpected overloading on scuffing initiation with a twin-disc test device. An existing twin-disc test device was modified to be suitable for applying overloading dynamically to the disc contact. Three test series including three pairs of discs in each series were subjected to combined normal force and rolling/sliding loading. First a base level for scuffing initiation was defined by increasing the normal load stepwise until failure, while keeping the rolling and sliding between the discs constant. In the subsequent test series, the overload cycles were applied at a significantly lower level in two different patterns leading to scuffing at both an earlier and later stage than was observed for the base level.

Keywords: Scuffing, twin-disc, overload, friction.

1. Introduction

Bevel gears in ship shafting lines often experience occasional overload cycles caused by propeller impacts on hard obstacles e.g. ice floes. The gear teeth have long been dimensioned against dynamic loads using load influence factors. However, occasional overload cycles are usually not noticed as a separate factor and therefore their role is neither visible nor accounted for in gear dimensioning.

The exact initiating mechanism of scuffing failure is not fully understood, although there appears to be a close relationship between a scuffing failure and lubricant film breakdown as noted in e.g. Ref. [1]. High surface pressure and sliding velocity with consequent frictional heating may affect the thickness of the lubrication film, whose decreasing viscosity leads to damaging asperity contact.

In addition, shear stresses play a key role in determining the film's thickness in an EHL contact between the rolling surfaces and the lubricant. However, a lubricant can only withstand a limited shear stress [2, 3]. If this limit is exceeded and if the maximum allowable shear stress in the oil is more dependent on the oil's temperature than viscosity, a thinner oil film may result because less oil is dragged into the contact area [4].

Another factor to consider is that a transient load rise instantly reduces the lubricant film thickness at the same time increasing the friction coefficient [5], which increases the potential for asperity contacts. It has also been reported that a temperature rise in the lubricant film profile occurs under heavy loading, due to the compression and the viscous friction [6, 7] increasing the risk for a scuffing failure.

The risk of scuffing is also known to be high during the initial settling of contacting surfaces often termed 'running-in', which is defined as the series of processes of wear rate and friction stabilisation for lubricated contacts [8]. In fact, the nature of scuffing is different than other gear failure modes in that it may be initiated after only a short period of severe load cycles in harsh conditions. Hence, rarely occurring occasional overload cycles may shorten the gear's life time significantly through a scuffing failure.

The flash temperature method is a widely-used approach to calculate the risk of scuffing. It was originally proposed by Blok [9] in 1937 and further enhanced by Jaeger [10] and Archard [11]. The basis of the theory is in the calculation of

Published article can be found at: https://doi.org/10.1016/j.triboint.2017.01.005

the maximum contact temperature t_c, which is an indication of the risk for a scuffing failure. This temperature is considered to be the sum of the bulk temperature t_b and the flash temperature t_{fmax} generated in the contact as follows:

$$t_c = t_b + t_{f\max} \tag{1}$$

One of the challenges with the above theory is the evaluation of the bulk temperature. In many cases this can be found by measurement, but an analytical approach based on loading is presented in Ref. [12]. Also recently Xue et al. proposed a method for predicting scuffing failure in spur gear pairs by means of a transient thermal solver [7]. This includes a temperature rise formula based on transient heat flux and a transient thermal elastohydrodynamic lubrication (TEHL) model, which takes into account the dynamic loads.

The experimental approach for finding the scuffing load-carrying capacity of a lubricant-material pair is traditionally defined by conducting FZG test procedures described in the standards [13]. Additionally, several scuffing studies have been performed with both the FZG device [1] and with bevel-gear-based test devices [14, 15]. The focus has been on variating the used lubricant, the influence of the oil temperature and the applied loading, amount of the oil supplied and the effect of a coating on the contact surface. Despite the stability of the results delivered, the possibilities for investigating a wider range of parameters is somewhat limited; often requiring a new design for the gear wheels. In addition, several scuffing studies have been performed by variating the above mentioned parameters, but observing the behaviour of a piston ring and liner contact [16, 17, 18]. However, an obvious difference exists between the conditions in comparison to a gear teeth contact.

A new approach to the scuffing test has recently been presented [19]. This utilises a ball-on-disc test device with contra-rotating surfaces to limit the EHD films. This arrangement enables the determination of the boundary lubrication conditions over a wide range of sliding speeds.

With the twin-disc test device, the elliptical pressure distribution, which is seen between the gear teeth in e.g. spiral bevel gears, can be reproduced [20, 21]. This is done through the precise definition of the discs' geometries. Furthermore, the structure of the device enables the actual loading of the contact to be highly adjustable. Over the years, the twin-disc test device has been used to study the behaviour of friction, pitting formation, wear prediction and the influence of surface roughness [22, 23, 24, 25]. The effect of different surface conditions on scuffing initiation has been also investigated [26]. However, there has not been much research focusing on the effect of variable loading on scuffing failures, which is the main topic of this paper. The paper presents the first result of an investigation of the relationship between overload cycles and the initiation of scuffing using a twin-disc test device.

2. Test equipment

The tests are conducted with an existing in-house-built twin-disc test device as shown in Fig. 1. The original version of the device is described in detail in Ref. [27]. However, the device was updated in order to be able to apply dynamic loading on the contact. The hydraulic cylinder and its control valve, which place a variable normal force F_N on the discs, were renewed. In addition, the valve control system hardware has been updated and reprogrammed. The load frame with the test discs are illustrated in Fig. 2. The applied normal load is measured with a force transducer situated behind the normal force cylinder and its signal is used as an input for the valve controller.

The adjustable rotation speed, direction and slide-to-roll ratio are controlled with frequency converters, which drive the electric motors. These are joined to the shafts via couplings allowing minor misalignment between the axles.

Published article can be found at: https://doi.org/10.1016/j.triboint.2017.01.005

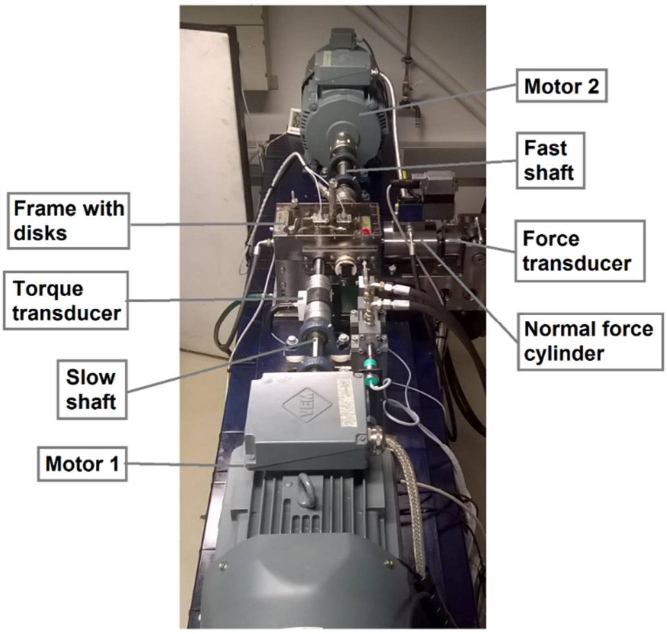

Fig. 1. The twin-disc test device.

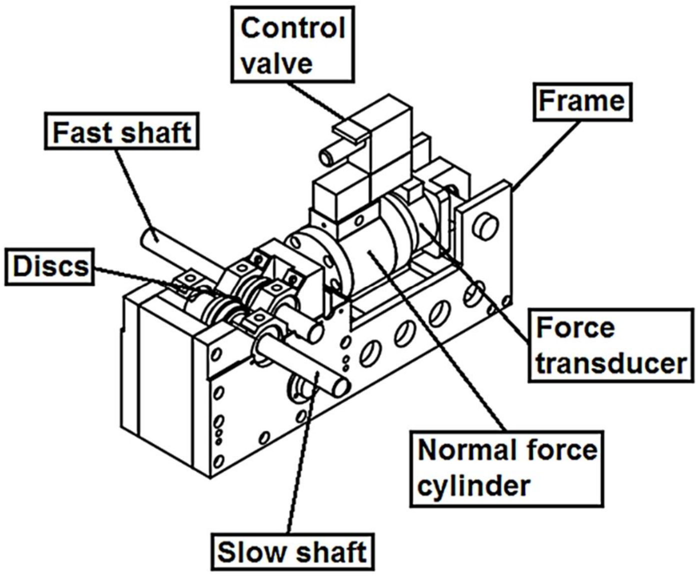

Fig. 2. The load frame.

A separate hydraulic unit provides lubricant for the disc contact injected from the inlet side. The same unit also lubricates the support rolling bearings inside the test device. Stepless adjustment of the lubricant flow is provided by means of a frequency-converter-driven pump motor and manual valves. The lubricant inlet temperature is automatically controlled by a separate microcontroller unit.

Published article can be found at: https://doi.org/10.1016/j.triboint.2017.01.005

The test device is highly adjustable and automated enabling the possibility for unmanned operation. Some of the performance values are listed below:

- Rotation speed: Max 6000 RPM
- Normal load: Max 50 kN
- Lubricant temperature: 25…120 °C
- Lubricant flow rate: 0.5…20 l/min

2.1. Measurements

The measurement system collects data on the above-mentioned normal force, lubricant flow and inlet temperature, as well as the shaft rotation speeds and the torque on the slow shaft. In addition, the test disc bulk temperature on the fast shaft was recorded using a telemetry system and a thermocouple located approximately 3.5 mm underneath the surface at the disc contact.

The torque signal T_m measured by the torque transducer mounted on the slow shaft, can be separated into the torque T_r originating from the bearings and the shaft seals, and the torque T_c, which originates from the disc contact. These two values have to be separated in order to analyse the contact behaviour more precisely. The actual torque at the disc contact can be calculated with the following equation:

$$T_c = T_m \pm T_r \tag{2}$$

The T_r value is negative, when measuring the braking torque on the slower shaft and positive in the opposite situation.

Typical values for the torque T_r were found by measuring the shaft torque as a function of the normal force. This was done by rotating the shafts with the same speeds 175.8 RPM, resulting in a pure rolling condition. The operating temperature was 60 °C and three different disc pairs were used. A load-dependent equation was fitted to the measured values shown in Fig. 3:

$$T_r = 0.0801 \cdot \ln(F_N) - 0.0265 \tag{3}$$

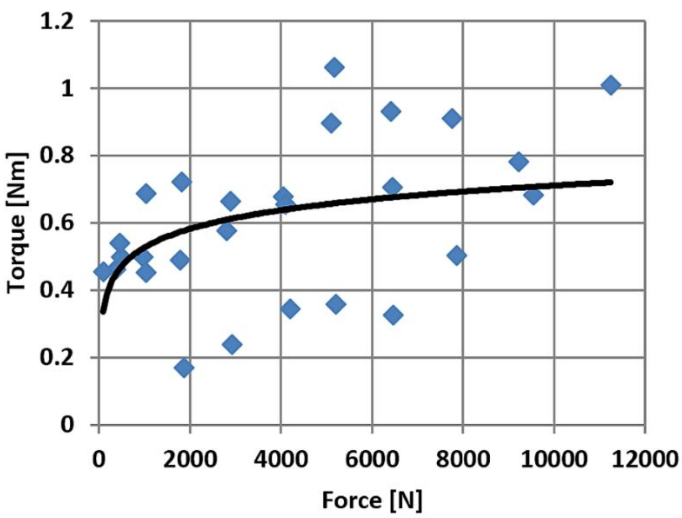

Fig. 3. Measured points of the torque T_r as a function of the normal force with a fitted curve according to Eq. 3.

The results, as illustrated in Fig. 3, show clear variation between an interesting normal force range of 5 to 12 kN. Hence, a sensitivity check was performed. This was done in two stages utilising the following equation:

Published article can be found at: https://doi.org/10.1016/j.triboint.2017.01.005

$$\mu_c = \frac{T_m + T_r}{r_{disc} \times F_N} \tag{4}$$

Firstly, the torque T_m was calculated with a friction coefficient μ_c of 0.03 in disc contact, a disc radius r_{disc} of 0.035 m and by estimating the T_r with Eq. (3). Then the variation in the friction value was evaluated by setting the torque T_r first to 0.4 Nm and then to 1.0 Nm. The used friction value of 0.03 represents a typical value according to the experiments and the used T_r values were found in Fig. 3. The results in Fig. 4 show a corresponding error range in the friction coefficient. The height of the friction error band is found to be insignificant, being roughly from 0.003 to 0.001 depending on the normal force.

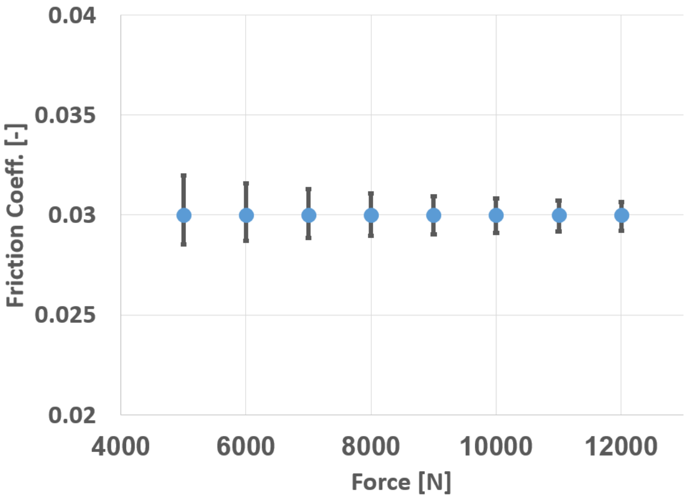

Fig. 4. Calculated error bands due to variation in measured torque originating from bearings and seals.

The values found with Eq. (3) were used for all the test runs since the bearings, seals and their lubrication do not change.

3. Test specimen and lubricant properties

The discs are 70 mm in diameter and the width of the contacting surfaces is 10 mm. In an axial direction the radius is set to 100 mm on the fast rotating disc while the other is flat. This allows an elliptical contact trace to be formed. The discs are turned from a round bar of 18CrNiMo7-6 (EN 10084) and case hardened to a surface hardness of 59-61 HRC

A special grinding device was designed for manufacturing the desired radius and a surface topography of a real gear-flank's surface. The basic principle of this device is to rotate the disc to be ground against a rotating grinding stone at a specified radius in order to produce perpendicular grinding marks on the specimen's surface, as shown in Fig. 5 and explained in detail in Ref. [27]. The discs were assembled on shafts before the final grinding in order to minimise any possible eccentricities of components arising from the manufacturing tolerances. The average surface finish (R_a) of both discs has to be between 0.28 and 0.32 µm and the average distance of the highest peak from the lowest valley (R_z) should be below 3 µm.

Published article can be found at: https://doi.org/10.1016/j.triboint.2017.01.005

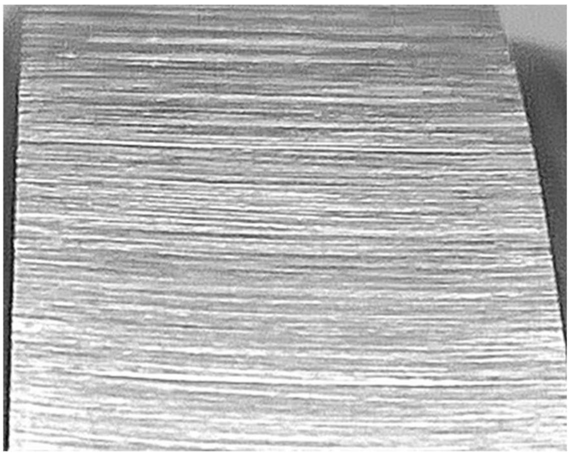

Fig. 5. Perpendicular grinding of a test specimen.

The lubricant is a mineral-based commercial gear oil with an EP-additive system for heavy duty industrial gears, which is commonly used in marine thruster systems. The oil's properties are shown in Table 1.

Table 1. Properties of the used lubricant according to the supplier.

		Value
Kin. viscosity @40ºC	[mm^2/s]	150
Kin. viscosity @100ºC	[mm^2/s]	15
Density @15ºC	[kg/m^3]	897
VG class	[-]	150
Flash point (COC)	[°C]	240
Pour point	[°C]	-24

4. Experimentation procedure and test cases

The experiments commenced with a pre-run, during which the shafts were rotated at the same low speed for about an hour with lubricant circulation and without normal load. During this time the lubricant and the temperature of both shafts were stabilized to a constant level.

For the actual test runs the shaft rotation speeds were adjusted in order to achieve a high surface sliding speed, which is known to increase the risk of a scuffing damage. The fast shaft rotated at 2039.3 RPM and the slow one at 175.8 RPM. With a specimen diameter of 70 mm this leads to a surface sliding speed of 6.8 m/s and a slide-to-roll ratio of 1.68. The relatively high sliding speed was determined by preliminary tests delivering scuffing failure at an achievable force level for a reasonable test duration.

The lubricant flow has an obvious effect on the temperature of the contact through heat energy transfer. However, its influence in real applications is often relatively challenging to predict. During the testing the oil flow to the contact inlet was 6 l/min, which according to the preliminary tests is an adequate oil supply providing clear bulk temperature increase after load rise. The lubricant inlet temperature was set to 60 °C, which can be considered as a typical value or slightly below average for the common temperature range of 40 °C to 100 °C used for industrial gears for power transmission applications [28]. These parameters were kept constant during the tests.

All the tests follow a common stepwise increasing normal load structure as shown in Fig. 6. The loading is increased after 1000 s at that particular load level. During this period aggressive asperities on contact surfaces are flattened and the specimen's temperature is simultaneously increased and stabilised at a higher level.

Published article can be found at: https://doi.org/10.1016/j.triboint.2017.01.005

The step magnitudes in Fig. 6 represents the Hertzian maximum contact pressure p_{max} for elliptical contact between the discs:

$$p_{\max} = \frac{3F_N}{2pab} \tag{5}$$

where a and b are the semimajor axes of the contact ellipse. The increases from zero to step 1 and from step 1 to 2 are somewhat larger than the other steps due to the current test setup's lower accuracy in force control with relatively low normal forces. The step increases from 2 to 6 are about 230 MPa per step and they are considered as running-in steps covering a running-in up to full loading of a newly-ground gear teeth in real-life applications. These steps allow the specimen's initial settling of the surfaces. During this period the temperature and the torque signals are stabilised. The scuffing failure and overload cycles are not applied until level 6 and upwards, which proceed in steps in 150 MPa.

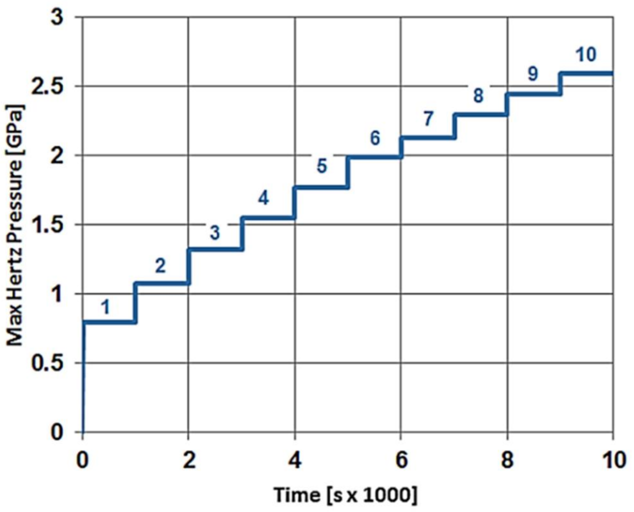

Fig. 6. First 10 steps of a stepwise loading structure for the scuffing tests.

The test matrix contains three different types of test runs:

A. **Reference** test
B. **Series of rapid sudden overload** cycles with high magnitude
C. **Series of sudden overload** cycles with increasing magnitude

For the reference test A, the stepwise load increase is continued until scuffing occurs. The purpose of this is to set the nominal level for failure initiation.

In series B the objective is to apply overload cycles instantly after the step increase i.e. during the stabilisation process. Fig. 7 shows an example of a series of overload cycles starting from level 7. The magnitude is set to reach level 9.

Series C is more aimed at the running-in process. The overloading begins at a clearly lower level than the scuffing level of the reference tests, but in contrast to the series B tests, the overload cycles are introduced to the system at steadily increasing rates. After stabilisation at the chosen level the first overload cycles are applied in magnitudes reaching to the next level. This 1000 s period is followed with another 1000 s period at the starting level, which in turn is followed with overload cycles one level higher than the previous ones. This procedure is repeated until scuffing occurs. An illustration of the procedure starting from level 7 is shown in Fig. 8.

Published article can be found at: https://doi.org/10.1016/j.triboint.2017.01.005

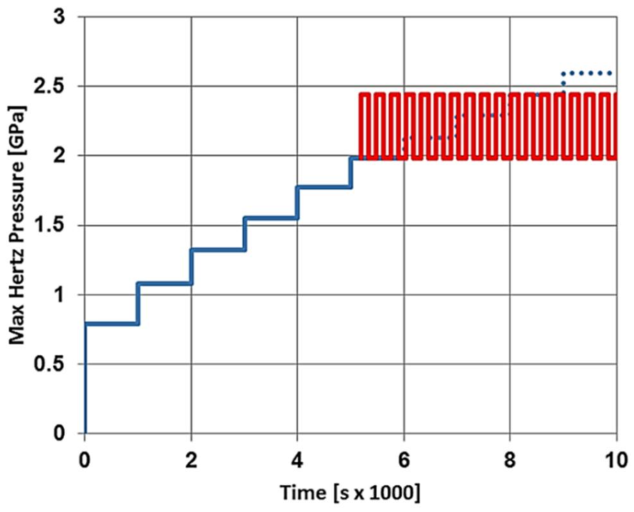

Fig. 7. Illustration of stepwise increasing overload cycle series of test series B. Series of overload cycles is applied after a series of nominal load cycles at the chosen level.

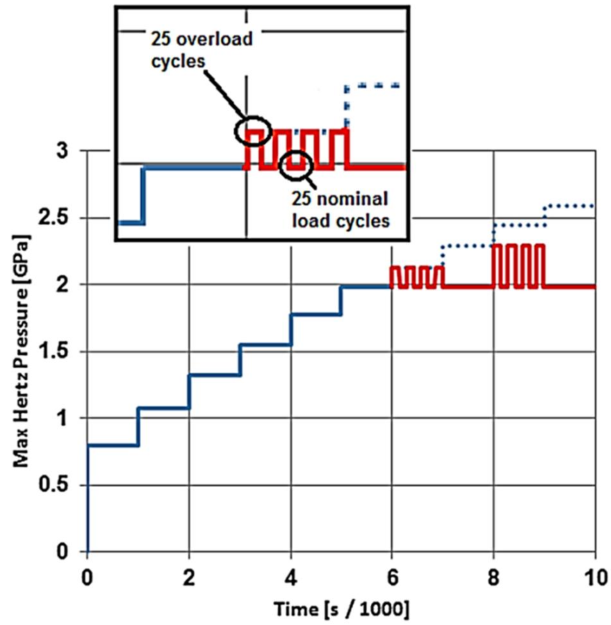

Fig. 8. Principle of stepwise increasing overload cycle of test series C. Each overload cycle regime is followed with a nominal load cycle regime at the particular level.

The actual overloading experienced by a ship's shafting line when that ship is sailing through icy seas for example, is challenging to reproduce. With its propeller constantly striking ice floes and the subsequent loading on the gear contacts, it is difficult to be certain what is actually going on in a real-life situation. In addition, the measurement data achieved from such a situation is often considered installation-specific, depending on the dynamic behaviour of the mechanical system. Therefore, only coarse estimate of potential loading schemes is utilised for both series B and C. The loading during the overloading period is always applied in a series of 25 + 25 cycles i.e. first at the specific overload level and then on the starting level.

The actual scuffing initiation is manifested as a rapid increase in the torque signal. This is regarded as a stop criterion for the testing.

Published article can be found at: https://doi.org/10.1016/j.triboint.2017.01.005

5. Results and discussion

Each test was repeated three times with the same loading scheme. The lubricant temperature at the contact inlet remained within the range of 60±1.5 ºC for all the tests.

The surface roughness for all the test specimens was measured at three locations on the test disc in circumferential direction at a distance of approximately 120 degrees. Table 2 presents the average of the three measurements for each test specimen, and it clear shows that there is a uniformity between the specimens.

The force and torque sensors were calibrated before, after and occasionally during each full test series with dead weights.

Table 2. Average surface properties for the ground test specimen.

Test	R_a [µm]	R_z [µm]	Radius [mm]
A1, curved	0.294	2.524	98.0
A1, flat	0.291	2.356	N/A
A2, curved	0.295	2.011	97.8
A2, flat	0.305	2.503	N/A
A3, curved	0.313	2.982	101.5
A3, flat	0.301	2.253	N/A
B1, curved	0.313	2.993	97.4
B1, flat	0.273	1.980	N/A
B2, curved	0.301	2.281	95.0
B2, flat	0.300	2.479	N/A
B3, curved	0.292	1.839	98.1
B3, flat	0.274	1.976	N/A
C1, curved	0.308	2.636	102.6
C1, flat	0.307	2.433	N/A
C2, curved	0.300	2.225	98.1
C2, flat	0.343	3.645	N/A
C3, curved	0.308	3.678	97.1
C3, flat	0.290	2.209	N/A

An example of resulting surface condition after scuffing failure is shown in Fig. 9. In the middle of the surface there can be seen a dark area with clearly visible wear grooves in circumferential direction, where the scuffing occurred.

Published article can be found at: https://doi.org/10.1016/j.triboint.2017.01.005

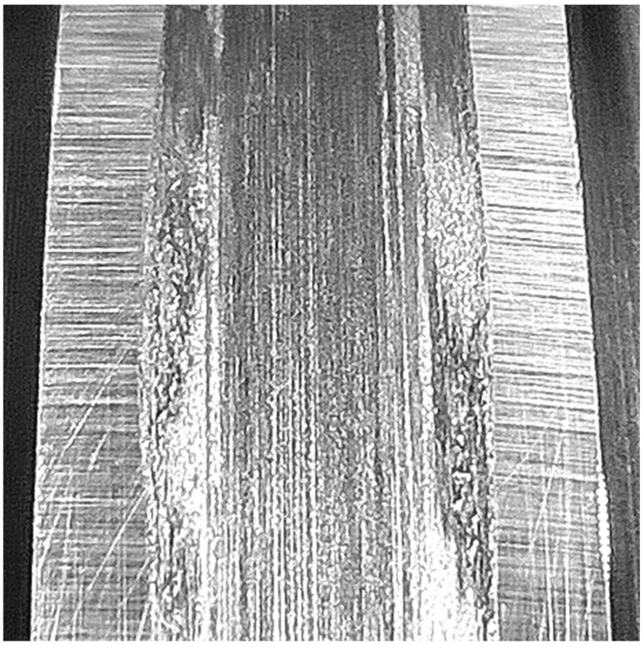

Fig. 9. Typical specimen surface after scuffing failure.

5.1. Scuffing failure

An averaging algorithm was applied on the actual measured signals. A moving average of changing length, depending on the observed load step, was calculated for the series of data points over the full data set. This was done in order to remove any electrical distortion caused by the measurement equipment and/or geometrical imprecision originating from the manufacturing tolerances or deformation of the components. The oscillation around the average for normal force was from ±1.5…±5 %, which corresponds to ±0.5…±1.7 % in maximum Hertzian contact pressure just before scuffing occurred. The upper limit of ±1.7 % means there is a ±40 MPa oscillation in the maximum Hertzian pressure. This indicates that the step size of 150 MPa is enough to produce a distinct difference between the steps.

In the torque measurements the oscillation was ±6…±8 % respectively. The upper limit of ±8 % leads to ±0.002 oscillation around the mean for the evaluated friction coefficient, which also shows that the tests are of sufficient accuracy.

The results from the test cases are shown in Table 3. The tests within each groups A, B and C are broadly the same, although there are minor differences between them. Case A3 was tested with a step length of 1500 s and reversed shaft speeds, i.e. the fast shaft was programmed to run at the slow shaft's speed, and vice versa. This experiment showed results in- line with A1 and A2. The starting level for the overload cycles for Case C1 was one level higher than for C2 or C3.

The amount of torque originating from the bearings and seals was calculated with Eq. 2. These values were subtracted from the measured signal in order to estimate the torque and friction between the discs at different loads. Typical result curves for the altered test types are shown in Figures 10, 11 and 12.

The newly ground surfaces, along with the torque from the bearings and shaft seals produce inaccuracies in the determination of the contact torque and the ensuing friction coefficient. These are between 0 and roughly 1000 s, as can be seen in Figures 10, 11 and 12. One reason for this is that the torque between the discs is at the same level as the torque rising from the bearings and seals. This leads to the partly labile behaviour of the system at low load levels.

Table 3. Measured normal force and bulk temperature with calculated maximum Hertzian pressure and friction coefficient between test specimen just before scuffing initiation.

Published article can be found at: https://doi.org/10.1016/j.triboint.2017.01.005

Test	Overload starting level	Scuffing level	Normal force [kN]	Bulk temperature [ºC]	Hertzian pressure [GPa]		Fric. coefficient [-]
					Max	Mean	
A1	N/A	10	9.67	178	2.59	1.73	0.022
A2	N/A	10	9.45	177	2.57	1.71	0.026
A3	N/A	10	9.73	175	2.60	1.73	0.022
B1	7	9	7.88	136	2.42	1.61	0.031
B2	7	9	7.89	133	2.42	1.61	0.030
B3	7	9	7.75	127	2.41	1.61	0.033
C1	8	13	15.0	-	3.00	2.00	0.023
C2	7	13	15.5	169	3.04	2.03	0.024
C3	7	11	11.6	159	2.76	1.84	0.024

5.1.1. Findings related to scuffing initiation

As Table 3 shows, in general, the initiation of scuffing requires high loads in terms of contact pressure and bulk temperature. Although the results show good repeatability within each test type, there are distinctive differences between the three series of tests, i.e. A, B and C. For example, in series B, with the overload cycles, the scuffing was initiated at a one-step lower load level and with about a 30 % lower bulk temperature than it was for series A. Since the friction coefficient in series B was approximately 30 % higher, the scuffing initiation may be explained by localised, instantaneous, high heat generation and subsequent high (flash) temperatures on the surfaces while they are settling. In this regard, Castro et. al. [29] have proposed an approach to predicting gear scuffing safety by dividing the analysis into global and local parts depending on the state of the running-in and the contact pressure.

A comparison of test series A and C shows that it is possible to apply loading up to 18 % higher in terms of maximum Hertzian pressure without initiating scuffing. This is calculated by comparing the highest levels without scuffing, i.e. 9 and 12 respectively, with corresponding max Hertzian pressures of roughly 2.45 GPa and 2.90 GPa, respectively. It is also worth of noting, that the bulk temperatures at the moment of scuffing initiation do not differ significantly. Therefore, and because of the lower scuffing level reached with test C3, a need for further research is obvious.

When looking at the utilized normal forces, the most interesting difference can be seen between series B and C. If C3 is discounted, the required force for scuffing is nearly 94 % higher in series C than it is in series B, and about 58 % higher than in series A.

Table 3 shows that the bulk temperature measurement can only provide a rough estimate of scuffing initiation. The gear's loading history and its consequent surface condition have a significant impact on the development of a scuffing failure. The effects of these factors on the calculation methods for evaluating scuffing risk will be studied in more in detail in the near future.

5.1.2. The effect of sudden overload cycles

According to the test results in Figs. 10, 11 and 12, each increase in the load is followed by a settling period of about 200 to 400 s most clearly manifested at 4000 to 7000 s as a reduction in the torque signal. The risk of scuffing seems to be high during this period of stabilization. A comparison of series A and B shows that although an increase of about 150 MPa in the maximum Hertzian contact pressure is not damaging, 300 MPa during the settling period clearly leads to failure under high loading conditions.

However, if the contacting surfaces are run-in properly, an overload of roughly 450 to 750 MPa can be tolerated. This tendency is clearly shown in the results from test series C, despite of the deviations due to local surface roughness or material variation.

Published article can be found at: https://doi.org/10.1016/j.triboint.2017.01.005

5.1.3. The evolution of friction

The friction coefficient rises along with the load from 1000 seconds until it reaches a turning point at between 3000 and 4000 sec. Thereafter the friction begins to decline as shown in Figures 10, 11 and 12.

During the first period, the development of friction is dominated by increasing viscosity along with the loading as well as by asperity contacts in the mixed lubrication region as the flattening of the contacting surfaces progresses. Once the test set-up is at the level of ~1550 MPa in maximum Hertzian contact pressure, there is a clear change in the process as the friction begins to decline. There are two possible scenarios, or combination of them, which could explain this. The first is that at this point the aggressive asperities are considerably levelled and the system is moving towards an elasto-hydrodynamic lubrication regime, where the definition of the friction coefficient is dictated by the shear stresses in the lubricant. This period is characterised by the tendency of the friction coefficient to slightly drop along with increases in the load. This produces a consequent reduction in the lubricant's limiting shear stress along with the increasing temperature, as noted in Ref. [30]. It is also noticeable that during this period the introducing of overload cycles has no significant effect on the friction coefficient. In the second scenario, the additive system of friction improvers in the lubricant become active, which would also have a strong influence on the system's behaviour.

5.1.4. The evolution of the bulk temperature

The bulk temperature climbs to a new level after each step-increase in the load, as shown in Fig. 13. This is due to an increase in the generation of frictional heat in the contact. After reaching the local maximum, in roughly 300 seconds, the heat production and the cooling via the transfer of heat energy within the lubricant and to the surrounding structures stabilizes. A small drop in the temperature can be observed, indicating a reduction of the friction coefficient. This is also supported by a simultaneous drop in the torque signal.

The comparison of the temperature curves for tests A1 and C3 in Fig. 13 show, that for example between 7000 and 8000 s the overload-type of loading to one step upper level produces approximately half of the temperature rise that it does under full-time loading on this level. After stabilisation and return to full-time loading at the previous load level with the overload procedure, the bulk temperature is observed to be declining, which indicates reduction in corresponding friction. This trend seems to continue during the process of applying the overload cycles in series C. This suggests that the heat generation can be kept under control, decreasing the risk of scuffing, without losing the advantage gained from the surface flattening with this procedure.

Published article can be found at: https://doi.org/10.1016/j.triboint.2017.01.005

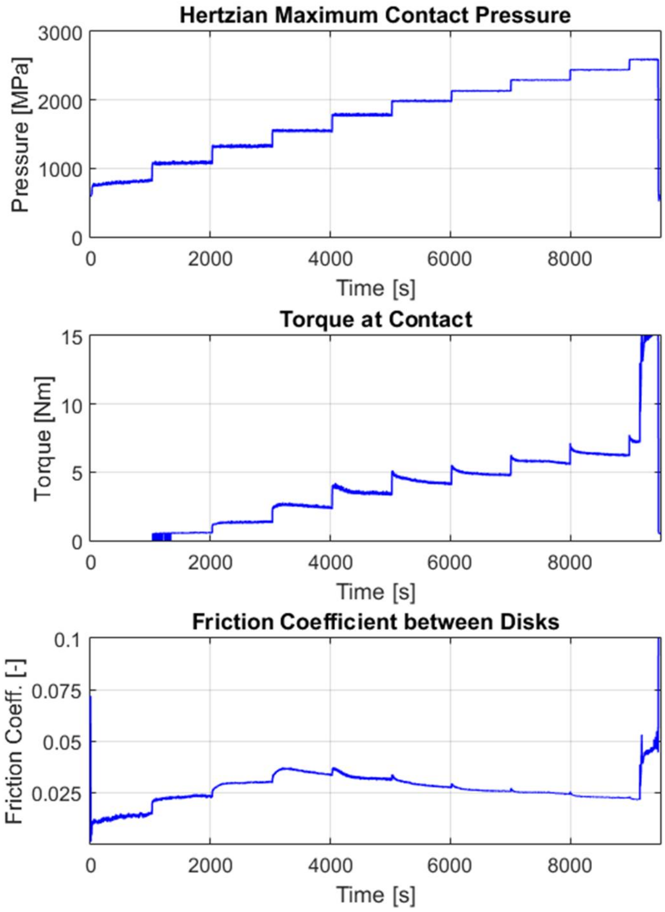

Fig. 10. Calculated Hertzian maximum contact pressure, torque at the contact and friction coefficient between the discs for test A1. Scuffing is initiated after step increase at 9000 s.

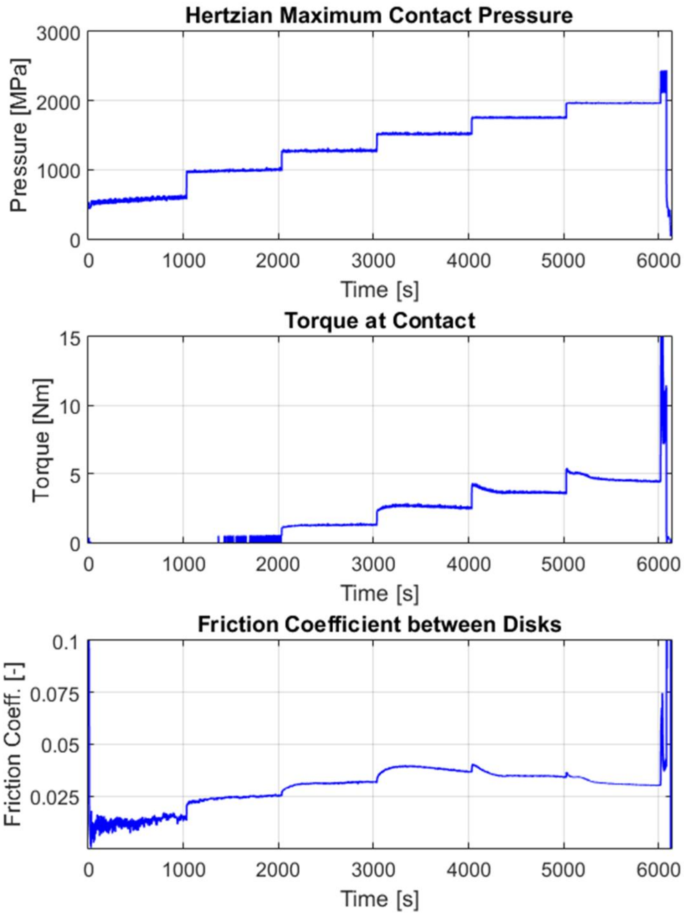

Fig. 11. Results for test B1. Series of overload cycles are applied after step increase at 6000 s leading to scuffing failure.

Published article can be found at: https://doi.org/10.1016/j.triboint.2017.01.005

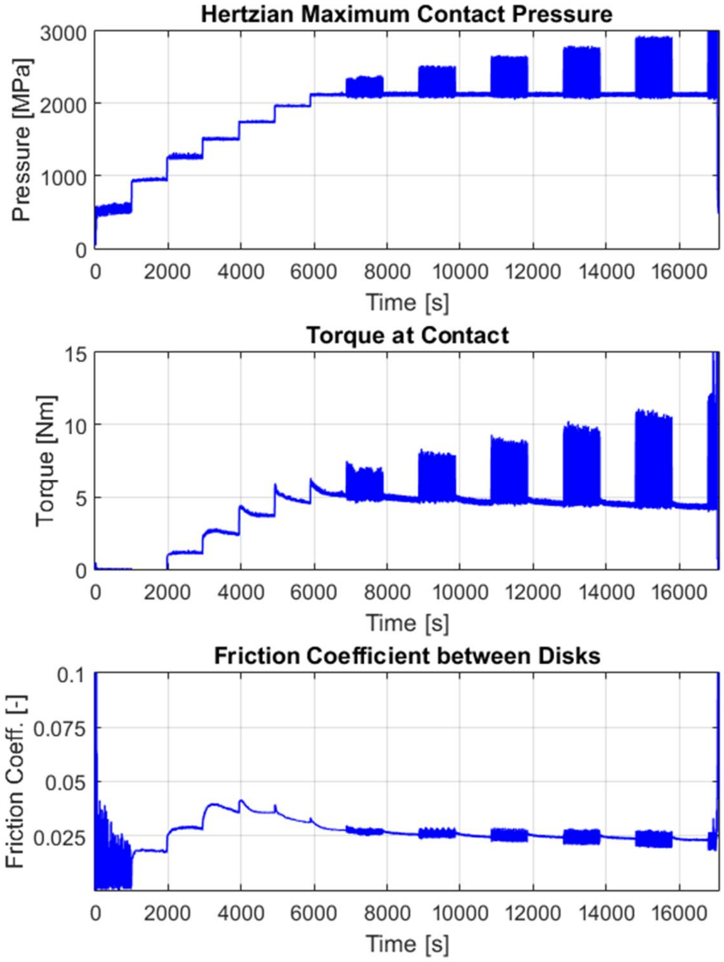

Fig. 12. Results for test C2. Series of overload cycles are visible in all the curves. Scuffing initiation occurs in the beginning of the 5th series.

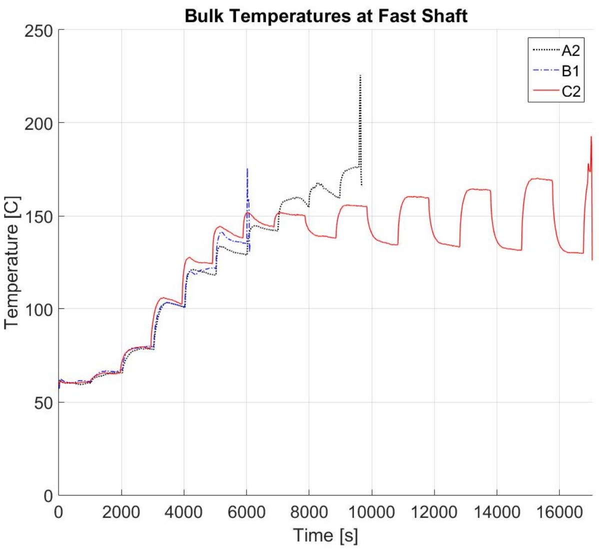

Fig. 13. Bulk temperature for test cases A2, B1 and C2. Scuffing initiation is seen as a rapidly rising peak in the temperature signal.

Published article can be found at: https://doi.org/10.1016/j.triboint.2017.01.005

6. Conclusions

This paper has presented the results of an approach to investigating scuffing initiation under overloading by means of a twin-disc test device. The main conclusions can be summarised as follows:

- The twin-disc test arrangement is well suited to study scuffing under dynamic loading.
    - The mechanical and thermal loads are efficiently controlled and their influence on the behaviour of the lubrication film are well captured.
    - A wide range of applied loads and surface conditions as a result of running-in can be studied effectively.
- Scuffing initiation due to overloading is substantially dependent on the occurrence of the loading.
    - Overload cycles during the running-in period significantly increase the risk for scuffing.
    - The introduction of overload cycles in a controlled manner, taking into account the settling of the surfaces and the increase in surface temperature, may improve the component's resistance to scuffing initiation under heavy loading.
    - The load history of the gears and their subsequent surface condition caused by running-in have a considerable effect.
- Using the bulk temperature to predict the risk of scuffing in a material-lubricant pair only gives a rather coarse result.

The improved performance against scuffing failure gained by introducing overloading is not only dependent on the magnitude of the applied load cycles or the sequence, but the prevalent temperature and the contact pressure. In addition, also other variables such as the gear's material, its initial surface condition and the lubricant, which impacts were not studied within the tests, may have a clearly noticeable effect. Because of this complexity, further research is required to enable the results of these tests to be utilised in dimensioning and more precise calculation of the risk for scuffing. In practice the achieved knowledge could be also applied to, for example, running-in processes of gears in marine applications.

7. Acknowledgements

This study is carried out under the auspices of the ArTEco (Arctic Thruster Ecosystem) project, which is part of the Maritime Technologies II Research Programme (MARTEC II) under the European Commission ERA-Net scheme. The authors wish to gratefully acknowledge financial support from Tekes and other partners in the project. The funders have had no influence on the content of this paper.

References

[1] Castro J, Seabra J. Scuffing and lubricant film breakdown in FZG gears. Part I. Analytical and experimental approach. Wear 1998;215;104-13.
[2] Jacobson BO. On the lubrication of heavily loaded spherical surfaces considering surface deformations and solidification of the lubricant. Acta polytechnic scandinavica, Me 54; Stockholm; 1970.
[3] Bair S, Winer WO. Lubricant shear response to large strain at high pressure. J. of Rheology 1980;6;936-7.
[4] Jacobson BO. Rheology and elastohydrodynamic lubrication. Elsevier tribology series, 19; Amsterdam, The Netherlands; Elsevier; 1991.
[5] Mongkol M, Jesda P. Transient EHL of two surfaces under elliptical contact with non-Newtonian lubricant. Advanced materials research 2012;452-453;1291-5.
[6] Bobach L, Beilicke R, Bartel D, Ludger, D. Thermal elastohydrodynamic simulation of involute spur gears incorporating mixed friction. Tribol Int 2012;48;191-206.

Published article can be found at: https://doi.org/10.1016/j.triboint.2017.01.005

[7] Xue J-H, Li W, Qin C. The scuffing load capacity of involute spur gear systems based on dynamic loads and transient thermal elastohydrodynamic lubrication. Tribol Int 2014;79;74-83.

[8] Hutchings IM. Tribology: Friction and wear of engineering materials. Butterworth-Heinemann; 1992.

[9] Blok H. General discussion on lubrication. Inst of Mech Eng 1937;2; London.

[10] Jaeger JC. Moving sources of heat and the temperature at sliding contacts. Proc Roy Soc N.S.W 76, 1942; 203-24.

[11] Archard JF. The temperature of rubbing surfaces. Wear 1959;2;438-55.

[12] Jiang QY, Barber GC. Experimental determination of bulk temperature and critical temperature in scuffing resistance evaluation of gears. Tribology transactions 2000;43;21-6.

[13] ISO 14635-1, -2, -3. Gears – FZG test procedures – Parts 1-3; 2012.

[14] Tuszynski W, Kalbarczyk M, Michalak M, Michalczewski R, Wieczorek A. The Effect of WC/C Coating on the Wear of Bevel Gears used in Coal Mines. Materials Science-Medziagotyra 2015; 21/3;358-63.

[15] Conrado E, Höhn B, Michaelis K, Klein M. Influence of oil supply on the scuffing load-carrying capacity of hypoid gears. Proceedings of the Institution of Mechanical Engineers 2007;221;851-8.

[16] Olander P, Jacobson S. Scuffing Resistance Testing of Piston Ring Materials for Marine Two-Stroke Diesel Engines and Mapping of the Operating Mechanisms. Wear 2015;330-331;42-8.

[17] Olander P, Eskildsen SS, Fogh JW, Hollman P, Jacobson S. Testing Scuffing Resistance of Materials for Marine 2-Stroke Engines - Difficulties with Lab Scale Testing of a Complex Phenomenon. Wear 2015;340-341;9-18.

[18] Obert P, Müller T, Füsser HJ, Barterl D. The influence of oil supply and cylinder liner temperature on friction, wear and scuffing behaviour of piston ring cylinder liner contacts – A new model test. Tribol Int 2016;94;306-14.

[19] Ingram M, Hamer C, Spikes H. A New Scuffing Test using Contra-Rotation. Wear 2015;328-329;229-40.

[20] Kleemola J, Lehtovaara A. An approach for determination of lubricant properties at elliptical elastohydrodynamic contacts using a twin-disc test device and a numerical traction model. Proceedings of the Institution of Mechanical Engineers 2008;222;797-806.

[21] Simon V. Load Distribution in Spiral Bevel Gears. ASME. J Mech Des 2006;129(2):201-9. http://dx.doi.org/10.1115/1.2406090.

[22] Kleemola J, Lehtovaara A. Experimental evaluation of friction between contacting discs for the simulation of gear contact. TriboTest 2007;13(1);13-20.

[23] Johansson J. On the influence of gear oil properties on pitting life. Dissertation, Luleå University of Technology, Luleå Sweden; 2015.

[24] Tassini N, Quost X, Lewis R, Dwyer-Joyce R, Ariaudo C, Kuka N. A numerical model of twin disc test arrangement for the evaluation of railway wheel wear prediction methods. Wear 2010;268;660-7.

[25] Höhn B-R, Michaelis K, Kreil O. Influence of surface roughness on pressure distribution and film thickness in EHL-contacts. Tribol Int 2006;39;1719-25.

[26] Snidle RW, Dhulipalla AK, Evans HP. Scuffing performance of a hard coating under EHL conditions at sliding speeds up to 16 m/s and contact pressures up to 2.0 GPa. J of Tribology 2008;130.

[27] Kleemola J, Lehtovaara A. Development of a high pressure twin disc test device for the simulation of a gear contact. Finnish Journal of Tribology 2006;25(2);8-17.

[28] AGMA 925-A03. Effect of lubrication on gear surface distress 2003.

[29] Castro J, Seabra J. Global and local analysis of gear scuffing tests using a mixed film lubrication model. Tribol Int 2008;41;244-55.

[30] Spikes HA. Mixed lubrication: an overview. Lubrication Science 1997;9;221-53.